PROCEEDING

Monitoring of IP₃ dynamics during Ca²⁺ oscillations in HSY human parotid cell line with FRET-based IP₃ biosensors

Akihiko Tanimura, Takao Morita, Akihiro Nezu, and Yosuke Tojyo

Department of Pharmacology, School of Dentistry, Health Sciences University of Hokkaido, Hokkaido, Japan

Abstract : Inositol 1,4,5-trisphosphate (IP₃) is an intracellular messenger that elicits a wide range of spatial and temporal Ca²⁺ signals, and this signaling versatility is exploited to regulate diverse cellular responses. In the present study, we have developed a series of IP₃ biosensors that exhibit strong pH stability and varying affinities for IP₃, as well as a method for the quantitative measurement of cytosolic concentrations of IP₃ ([IP₃]ᵢ) in single living cells. We applied this method to elucidate IP₃ dynamics during agonist-induced Ca²⁺ oscillations, and demonstrated cell type-dependent differences in IP₃ dynamics ; a non-fluctuating rise in [IP₃]ᵢ and repetitive IP₃ spikes during Ca²⁺ oscillations in COS-7 cells and HSY-EA1 cells, respectively. The size of the IP₃ spikes in HSY-EA1 cells varied from 10 to 100 nM, and the [IP₃]ᵢ spike peak was preceded by a Ca²⁺ spike peak. These results suggest that repetitive IP₃ spikes in HSY-EA1 cells are passive reflections of Ca²⁺ oscillations, and are unlikely to be essential for driving Ca²⁺ oscillations. The novel method described herein as well as the quantitative information obtained by using this method should provide a valuable and sound basis for future studies on the spatial and temporal regulations of IP₃ and Ca²⁺. J. Med. Invest. 56 Suppl. : 357-361, December, 2009

INTRODUCTION

Inositol 1,4,5-trisphosphate (IP₃) is an important intracellular messenger produced by phospholipase C (PLC)-dependent hydrolysis of phosphatidyl-inositol 4,5-bisphosphate (PIP₂). IP₃ releases Ca²⁺ from intracellular stores *via* IP₃ receptors (IP₃Rs), and the resulting Ca²⁺ signals often exhibit complex spatial and temporal organizations, such as Ca²⁺ oscillations (1). The mechanism responsible for Ca²⁺ oscillations has been a long-standing question, and a number of experimental approaches and mathematical models have been reported to account for these Ca²⁺ signals, yet the mechanism responsible remains controversial (2). There are two general classes of Ca²⁺ oscillation. In one class, Ca²⁺ oscillations are generated in the presence of constant cytosolic IP₃ concentrations ([IP₃]ᵢ) (3) ; in the other class, oscillating [IP₃]ᵢ are required to drive Ca²⁺ oscillations (4).

In the present study, we developed a series of improved IP₃ biosensors which exhibit high pH stability and varying IP₃ affinities. They also possess higher selectively and afford a larger dynamic range than that of the original biosensor LIBRA. In combination with these new biosensors, we developed a method for quantitating IP₃ dynamics in single living

cells, and applied this method to measure IP₃ dynamics during Ca²⁺ oscillations.

RESULTS AND DISCUSSIONS

Characterization of improved IP₃ biosensors

Fig. 1A shows schematic diagrams of IP₃-biosensor domain structures. To improve the pH-stability of the LIBRA emission ratio (480 nm/535 nm), EYFP (enhanced YFP) was replaced with Venus, a pH-stable YFP mutant (5). The resulting construct (LIBRAvIII) showed strong pH stability in the range of pH 6 to pH 8 (Fig. 1B). Next the LIBRAvIII ligand-binding domain was replaced with that of type 1 or type 2 IP₃R, to create high-affinity IP₃ biosensors. These constructs were designated LIBRAvI

and LIBRAvII, respectively. It is known that changing Arg to Gln at position 441 (R441Q) increases the affinity of type 1 IP₃R (6). To further increase the affinity, comparable amino acid substitutions in type 2 and type 3 IP₃Rs (R440Q) were made in LIBRAvII and LIBRAvIII. We also generated IP₃-insensitive LIBRAv (LIBRAvN) by substituting Ala for Lys at position 508 (K508A) in the IP₃-binding domain of LIBRAvIII. These biosensors were distributed on the plasma membrane and in vesicular structures (Fig. 1C), and most of the associated fluorescence (>90%) was retained after permeabilization.

Concentration-response curves of the new IP₃ biosensors for IP₃, inositol 4,5-bisphosphate (IP₂) and inositol 1,3,4,5-tetrakisphosphate (IP₄) are shown in Fig. 1D. The apparent K_d (nM) of LIBRAvIII,
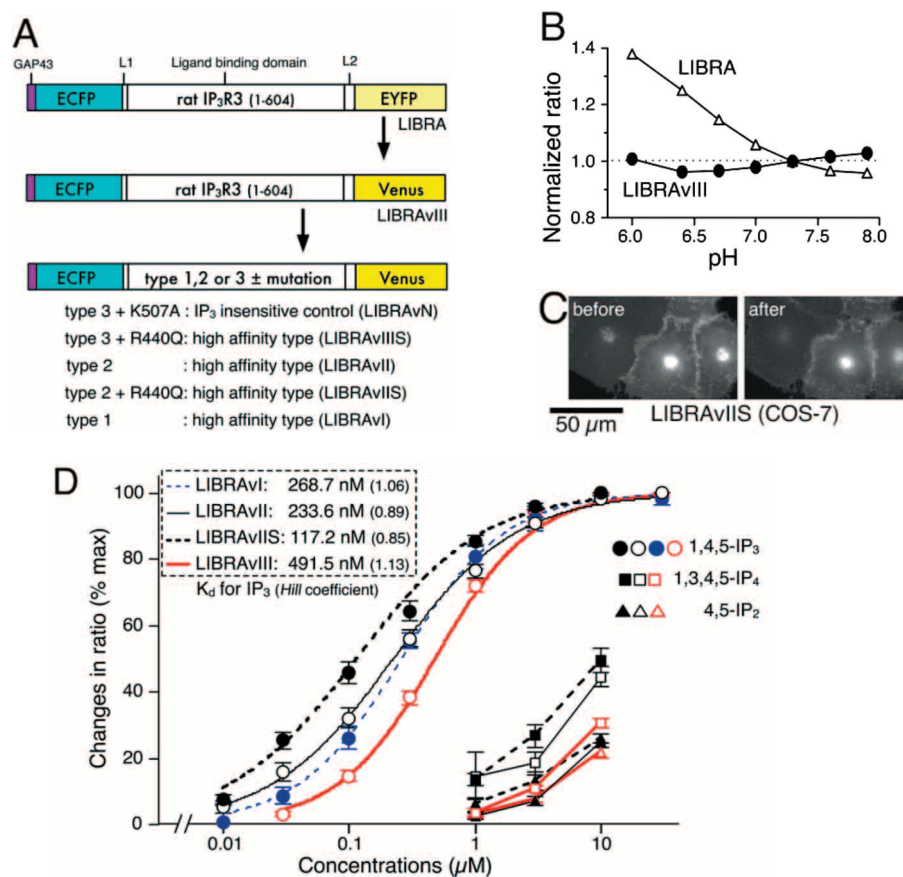

Figure 1. Characteristics of IP₃ biosensors.
(A) Schematic representations of domain structures of LIBRA and LIBRAv variants. IP₃ biosensors consist of a membrane-targeting signal (GAP43) ; the ligand-binding domain of rat IP₃R type 1, 2, or 3 (amino acids 1-604) ; ECFP, EYFP or Venus ; and linkers (L1 and L2). K507A and R440Q denote amino acids substitutions of the ligand-binding domain the IP₃R type 2 and 3. (B) Effects of pH on fluorescence emission ratios of LIBRA and LIBRAvIII. Emission ratios (480 nm/535 nm) of LIBRA and LIBRAvIII in permeabilized COS-7 cells were measured in ICM at various pHs. Emission ratios were normalized to the ratio at pH 7.3. (C) Fluorescent images of LIBRAvIIS-expressing COS-7 cells before and after permeabilization. (D) Concentration-response curves for inositol phosphates. Changes in emission ratio of LIBRAv variants due to exposure to various concentrations of IP₃ (circle), IP₂ (triangle), and IP₄ (square) were measured in permeabilized COS-7 cells (LIBRAvIII, LIBRAvII, and LIBRAvIIS) or in permeabilized HSY-EA1 cells (LIBRAvI). Changes in emission ratio were normalized to the effects of IP₃ saturation with 10 μM (for LIBRAvI, II, and IIS) or 30 μM (for LIBRAvIII) IP₃. Reproduced from ref. 5 with permission.

LIBRAvI, LIBRAvII, and LIBRAvIIS for IP$_3$ were 491.5, 268.7, 233.6, and 117.2, respectively. A high concentration (10 μM) of IP$_2$ or IP$_4$ induced 20~40% of the maximal response of these biosensors. LIBRAvII and LIBRAvIIS exhibited greater selectivity than LIBRA, and the selectivity of LIBRAvIIS for IP$_3$ was 300-fold higher than for IP$_2$ and 96-fold higher than for IP$_4$.

The characteristics of our IP$_3$ biosensors include the use of Venus, ligand-binding domains of different IP$_3$R isoforms, and a membrane-targeting signal. The superior selectivity of IP$_3$R-based FRET sensors provides a clear advantage over GFP-PHD sensors. In addition, utilizing Venus for a FRET-based biosensor is particularly important to avoid pH-related artifacts.

METHODS FOR QUANTITATIVE MEASUREMENT OF [IP$_3$]$_i$

Emission ratios of LIBRAvIII and LIBRAvIIS in intact cells increased upon the application of 10 μM ATP, and returned to basal levels after the addition of 5 μM U73122. To obtain the maximal changes in emission ratio in each individual cell, cells were permeabilized and exposed to IP$_3$ following the completion of measurements in intact cells.

The LIBRAvIII emission ratio did not change with U73122 treatment, whereas the LIBRAvIIS ratio decreased slowly to a new steady-state. These results indicate that the emission ratio of LIBRAvIIS reflects the resting [IP$_3$]$_i$, and U73122 decreases [IP$_3$]$_i$ to levels below the detectable range of LIBRAvIIS. Based on this idea, we used the U73122-induced decrease in emission ratios, K$_d$, and *Hill* coefficient of LIBRAvIIS (shown in Fig. 1D) to estimate the resting [IP$_3$]$_i$ in COS-7 and HSY-EA1 cells. U73122-induced decrease in emission ratio of LIBRAvIIS in COS-7 and HSY-EA1 cells was $13.67 \pm 0.96\%$ (Mean $\pm$ S.E., n = 60) and $16.03 \pm 1.53\%$ (n = 19), respectively. The estimated resting [IP$_3$]$_i$ in COS-7 and HSY-EA1 cells was 15.09 ± 1.38 nM and 18.16 ± 2.49 nM, respectively (5).

CHANGES IN [IP$_3$]$_i$ DURING AGONIST-INDUCED Ca^{2+} OSCILLATIONS

Resting [IP$_3$]$_i$ values allowed us to accurately calculate agonist-induced changes in [IP$_3$]$_i$. Figs. 2 shows changes in [IP$_3$]$_i$ during ATP-induced Ca^{2+}
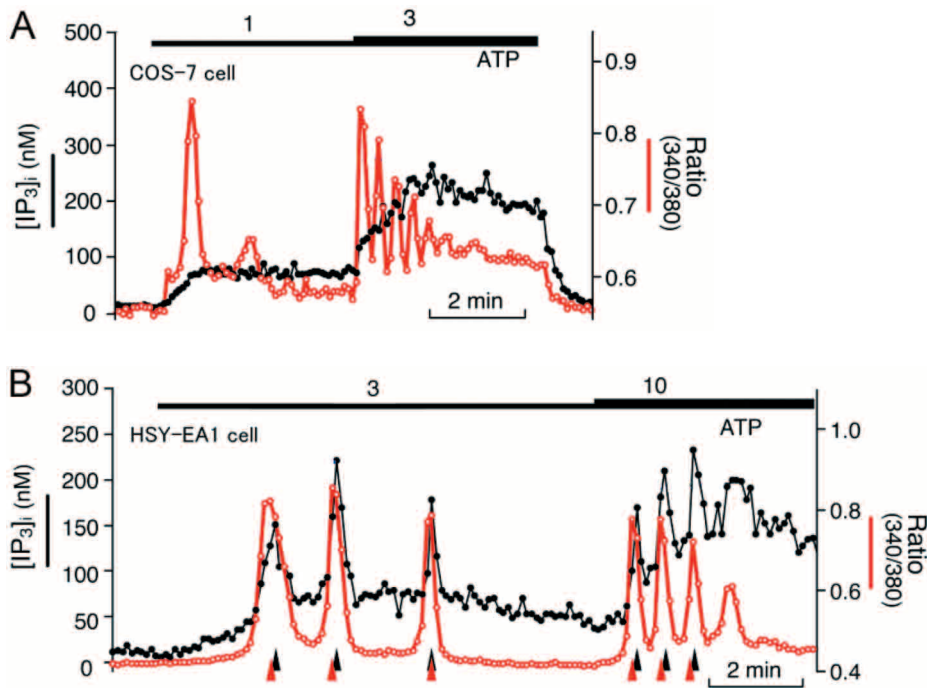

Figure 2. IP$_3$ dynamics during Ca^{2+} oscillations in COS-7 and HSY-EA1 cells.
LIBRAvIIS-expressing cells were loaded with fura-2, and sequentially stimulated with various concentrations of ATP. (A) COS-7 cells showed no detectable fluctuation in [IP$_3$]$_i$ during ATP-induced Ca^{2+} oscillations. Traces are representative of 27 oscillating cells. (B) HSY-EA1 cells showed repetitive IP$_3$ spikes during ATP-induced Ca^{2+} oscillations. Traces are representative of 31 out of 55 oscillating cells. Traces show estimated [IP$_3$]$_i$ (black lines), excitation ratio of fura-2 (red lines). Black arrowhead, peak of IP$_3$ spike ; red arrowhead, peak of Ca^{2+} spike. Reproduced from ref. 5 with permission.

oscillations. In COS-7 cells, stimulation with either 1 µM or 3 µM ATP increased $[IP_3]_i$ slowly to a sustained level without detectable fluctuations, and Ca^{2+} oscillations were observed during this increase and sustained elevation of $[IP_3]_i$ (Fig. 2A). Unlike ATP-induced increases in $[Ca^{2+}]_i$, the large increase in $[Ca^{2+}]_i$ caused by ionomycin (2 µM) treatment had no effect on the emission ratio of LIBRAvIIS, indicating that Ca^{2+} itself does not activate IP_3 generation in COS-7 cells (5).

We also examined IP_3 dynamics in HSY-EA1 cells (5). This cell line is characterized by long lasting Ca^{2+} oscillations in response to wide ranges of agonist concentrations (7). In fact, 65% of HSY-EA1 cells (55 out of 84 cells) exhibited Ca^{2+} oscillations following treatment with 3-100 µM ATP or 10-100 µM carbachol (CCh). Interestingly, 56% of Ca^{2+}-oscillating HSY-EA1 cells (31 cells) showed associated fluctuations in $[IP_3]_i$ (Fig. 2B). Similar fluctuations in the LIBRAvIIS emission ratio were observed when IP_3 dynamics were examined in the absence of fura-2 loading (data not shown). In contrast, no change in emission ratio was observed during Ca^{2+} oscillations in LIBRAvN-expressing HSY-EA1 cells. These experiments exclude the possibility of result artifacts derived from IP_3-independent changes in LIBRAvIIS fluorescence and possible interference by fura-2 fluorescence. These results demonstrate cell type-specific differences in IP_3 dynamics ; non-fluctuating rises in $[IP_3]_i$ and repetitive IP_3 spikes in COS-7 cells and HSY-EA1 cells, respectively. Quantitative examinations revealed that repetitive IP_3 spikes in HSY-EA1 cells occurred concomitantly with a slow basal accumulation of $[IP_3]_i$. The size of IP_3 spikes varied from 10 to 100 nM, and the second and later spikes were initiated before the decline of $[IP_3]_i$ to resting levels, resulting in a slow increase in the $[IP_3]_i$ interspike.

Although repetitive IP_3 spikes were observed in HSY-EA1 cells, our observations do not support the requirement of IP_3 fluctuations in Ca^{2+} oscillations. While $[IP_3]_i$ showed clear fluctuations at the beginning of Ca^{2+} oscillations, repetitive spikes of $[IP_3]_i$ gradually obscured during Ca^{2+} oscillations in 64% of HSY-EA1 cells. In addition, the $[IP_3]_i$ spike peak was preceded by a Ca^{2+} spike peak (Figs. 2B). These results suggest that repetitive IP_3 spikes in HSY-EA1 cells are passive reflections of the Ca^{2+} oscillations, and are unlikely to be essential for driving Ca^{2+} oscillations.

$[IP_3]_i$ fluctuations could be induced by the effects of Ca^{2+} on IP_3 synthesis and/or IP_3 degradation.

Applications of 2 µM ionomycin had little or no effect on the emission ratio of LIBRAvIIS in HSY-EA1 cells, suggesting that the direct effect of Ca^{2+} on IP_3 production is very small or absent in this cell line. Thus, $[IP_3]_i$ fluctuations are likely to be caused by Ca^{2+}-induced potentiation of agonist-dependent IP_3 generation. The IP_3 spikes described here resemble the pattern predicted by the oscillator model, in which positive feedback via Ca^{2+}-dependent activation of PLC is added to the dual positive and negative feedback effect of Ca^{2+} on IP_3R, rather than the model including negative feedback via Ca^{2+}-dependent IP_3-degradations by IP_3 3-kinases (8).

Ca^{2+} oscillations were observed primarily when $[IP_3]_i$ was less than 300 nM. More than 50% of COS-7 cells exhibited Ca^{2+} oscillations when $[IP_3]_i$ was 50-100 nM, and the percentage of oscillating COS-7 cells decreased as $[IP_3]_i$ increased. In HSY-EA1 cells, Ca^{2+} oscillations were observed in 50-70% of cells, when interspike $[IP_3]_i$ was less than 250 nM, and the percentage of oscillating cells decreased abruptly (11.1%) when interspike $[IP_3]_i$ was greater than 250 nM. These results indicate that low concentrations of IP_3 (< 100 nM) induce Ca^{2+} oscillations in both cell types, while HSY-EA1 cells are more likely to exhibit Ca^{2+} oscillations at higher concentrations of $[IP_3]_i$ (100-250 nM) than are COS-7 cells. Large increases in $[IP_3]_i$ (> 250 nM) induced the peak-plateau type Ca^{2+} response in both cell types.

The present study showed the time delay of IP_3 spike peaks from Ca^{2+} spike peaks in HSY-EA1 cells, and Ca^{2+} oscillations with non-fluctuations of $[IP_3]_i$ in COS-7 cells. Together these results suggest it is likely that IP_3 spikes are not essential to drive Ca^{2+} oscillations. Regarding the mechanism of Ca^{2+} oscillations, the importance of dual feedback effects of Ca^{2+} on IP_3Rs has been demonstrated experimentally (9-11). However, it has been pointed out that this dual feedback effect explains relatively short period Ca^{2+} oscillations but it cannot reproduce long interspike intervals. Thus, additional mechanisms responsible for establishing these oscillations remain unclear. One model study reported that frequency properties of oscillation are modulated by the incorporation of Ca^{2+} activation of PLC into the Ca^{2+} oscillation model based on dual feedback regulations of IP_3R properties, which enhances the range of frequency encodings of agonist stimulations (8). Interestingly, HSY-EA1 cells exhibited Ca^{2+} oscillations for a wider range of agonist and $[IP_3]_i$ concentrations than observed in COS-7 cells. Thus, it may be possible that repetitive IP_3 spikes or fluctuations play

some role in supporting and/or regulating Ca^{2+} oscillations. The quantitative information provided here would be useful for future studies of the mechanisms and roles of IP_3 oscillations.

REFERENCES

1.   Berrige MJ, Lipp P, Bootman MD : The versatility and universality of calcium signalling. Nat Rev Mol Cell Biol 1 : 11-21, 2000

2.   Dupont G, Combettes L, Leybaert L : Calcium dynamics : spatio-temporal organization from the subcellular to the organ level. Int Rev Cytol 261 : 193-245, 2007

3.   De Young GW, Keizer J : A single-pool Inositol 1,4,5-trisphosphate-receptor-based model for agonist-stimulated oscillations in Ca^{2+} concentration. Proc Natl Acad Sci USA 89 : 9895-9899, 1992

4.   Meyer T, Stryer L : Calcium spiking. Annu Rev Biophys Biophys Chem 20 : 153-174, 1991

5.   Tanimura A, Morita T, Nezu A, Shitara A, Hashimoto N, Tojyo Y : The use of FRET based biosensors for the quantitative analysis of inositol 1,4,5-trisphospate dynamics in calcium oscillations. J Biol Chem 284 : 8910-8917, 2009

6.   Yoshikawa F, Morita M, Monkawa T, Michikawa T, Furuichi T, Mikoshiba K : Mutational analysis of the ligand binding site of the inositol 1,4,5-trisphosphate receptor. J Biol Chem 271 : 18277-18284, 1996

7.   Tanimura A, Nezu A, Morita T, Hashimoto N, Tojyo Y : Interplay between calcium, diacylglycerol, and phosphorylation in the spatial and temporal regulation of $PKC\alpha$-GFP. J Biol Chem 277 : 29054-29062, 2002

8.   Politi A, Gaspers LD, Thomas AP, Höfer T : Models of IP_3 and Ca^{2+} oscillations : frequency encoding and identification of underlying feedbacks. Biophys J 90 : 3120-3133, 2006

9.   Wakui M, Potter BVL, Petersen OH : Pulsatile intracellular calcium release does not depend on fluctuations in inositol trisphosphate concentration. Nature 339 : 317-320, 1989

10. Tanimura A, Turner RJ : Inositol 1,4,5-trisphosphate-dependent oscillations of luminal $[Ca^{2+}]$ in permeabilized HSY cells. J Biol Chem 271 : 30904-30908, 1996

11. Hajnóczky G, Thomas AP : Minimal requirements for calcium oscillations driven by the IP_3 receptor. EMBO J 16 : 3533-3543, 1997